

## Structural origin of the colored reflections from the black-billed magpie feathers

Jean Pol Vigneron,<sup>1,\*</sup> Jean-François Colomer,<sup>2</sup> Marie Rassart,<sup>1</sup> Abigail L. Ingram,<sup>3</sup> and Virginie Lousse<sup>1,4</sup>

<sup>1</sup>Laboratoire de Physique du Solide, Facultés Universitaires Notre-Dame de la Paix, 61 rue de Bruxelles, B-5000 Namur, Belgium

<sup>2</sup>Laboratoire de résonance magnétique nucléaire, Facultés Universitaires Notre-Dame de la Paix, 61 rue de Bruxelles, B-5000 Namur, Belgium

<sup>3</sup>Natural History Museum, Cromwell Road, London SW7 5BD, United Kingdom

<sup>4</sup>Ginzton Laboratory, Stanford University, Stanford, California 94305, USA

(Received 12 October 2005; revised manuscript received 19 December 2005; published 27 February 2006)

The structural origin of the weak iridescence on some of the dark feathers of the black-billed magpie, *Pica pica* (Corvidae), is found in the structure of the ribbon-shaped barbules. The cortex of these barbules contains cylindrical holes distributed as the nodes of an hexagonal lattice in the hard layer cross section. The optical properties are described starting from a photonic-crystal film theory. The yellowish-green coloration of the bird's tail can be explained by the appearance of a reflection band related to the photonic-crystal lowest-lying gap. The bluish reflections from the wings are produced by a more complicated mechanism, involving the presence of a cortex second gap."

DOI: [10.1103/PhysRevE.73.021914](https://doi.org/10.1103/PhysRevE.73.021914)

PACS number(s): 42.66.-p, 42.70.Qs, 42.81.Qb

### I. INTRODUCTION

The black-billed (or common) magpie, *Pica pica* (Corvidae) is a very common bird. As many members of the Corvidae family, it is found over a very wide habitat and owns a broad feeding niche [1]. The common magpie distribution stretches from Europe to China and on, to Canada and Western United States. Magpies eat insects and small rodents, not neglecting eggs or fledglings of other birds. In Western America, these birds appear shy of humans, but their behavior in Europe is quite different. In Central and Western European regions, magpies are easily seen in the gardens of suburban areas, while, for instance, in northern Finland, their habitat overlap human settlements. The black-billed magpie appears at first glance as a boldly patterned bird with contrasted white and black plumage. However, under an appropriate light, iridescence can be perceived on many of its feathers (see Fig. 1). In particular, its long tail shows a yellowish-green iridescence on most of its length, with a bluish termination. On the wings, much of the dark areas show blue reflections.

The spectral filtering of diffused light by bird feathers is known, and generally explained by Tyndall scattering [2–4]. Bird feathers, however, can show much more complex optical properties, and these call for more complex mechanisms and more complex structures than simple isolated Mie scatterers. Light interference and diffraction [6,7] and even more collective mechanisms [5] can lead to iridescence. Recent evidences of these complex structures were found, for example, in the rose-faced lovebird (*Agapornis Roseicollis*) [8,9], and in the male peacock (*Pavo muticus*) [10].

In this paper, the origin of the iridescence of the feathers of the common magpie (*Pica pica*) is investigated, using reflectance measurements, scanning electron microscopy, theoretical modeling, and numerical simulations. As with the peacock feathers, the barbules that appear iridescent under

the optical microscope have a peripheral layer (the cortex" structured as a two-dimensional photonic crystal. But contrasting the case of *Pavo sp.*, this two-dimensional photonic crystal is here hexagonal, rather than rectangular [11], and the blue wing coloration is not determined by a mere reduction of the lattice parameter found in the greenish feathers.

### II. REFLECTANCE SPECTRA

The specular reflection from specific parts of intact feathers was investigated using an Avaspec 2048/2 fiber optic spectrometer. Measurements were performed under a normal incidence, collecting the backscattered light, using bifurcated optical fibers. By "normal incidence," we mean along the normal to the feather plane containing the shaft, the barbs, and the barbules. The results are shown on Fig. 2. The reflected intensity is expressed in units of the corresponding diffuse reflection obtained on a standard white diffusor. The sample which generated the data on Fig. 2 were taken on the



FIG. 1. (Color online) The black-billed magpie *Pica pica* is not exactly a black-and-white bird. This very common bird in Europe and Northern America has in fact yellowish-green iridescent feathers forming a long tail, and bluish reflections on the dark areas of the wings. Photograph courtesy of Thierry Tancrez.

\*Electronic address: [jean-pol.vigneron@fundp.ac.be](mailto:jean-pol.vigneron@fundp.ac.be)

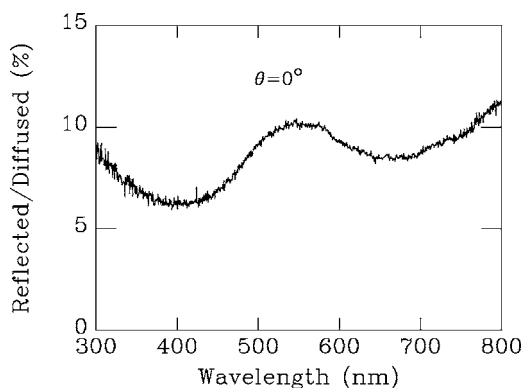


FIG. 2. Spectral distribution of the reflection of white light from yellowish-green iridescent feather of *Pica pica*, measured on the bird's tail. The reflectance spectrum is obtained at an incidence normal to the feather plane (incidence angle  $\theta=0$ ) (550 nm band).

yellowish-green part of the long tail feathers. The reflection is clearly centered, in the visible range, on a wavelength  $\lambda = 550$  nm. The spectral reflection band is however rather wide, extending from 500 nm to 600 nm. The reflected color is thus strongly desaturated. In dark regions of the body the level and variations of the reflectance are found to be rather weak. Much of the incident light is actually absorbed, so that under most ambient lights, this bird is perceived as essentially black and white.

The spectrum shown on Fig. 3 is relative to the blue iridescent feathers that can be found on part of the bird wings (see Fig. 1). As with the yellowish-green feathers, a back-scattering geometry was used at an incidence normal to the feather plane. The dominant wavelength is blue-shifted, compared to the band found on the tail feathers. This blue reflection band is also very wide. The dominant wavelength here is 460 nm.

### III. SCANNING ELECTRON MICROSCOPE VIEWS OF BARBULES

The examination of the iridescent feathers under an optical microscope shows that the coloration, when present,

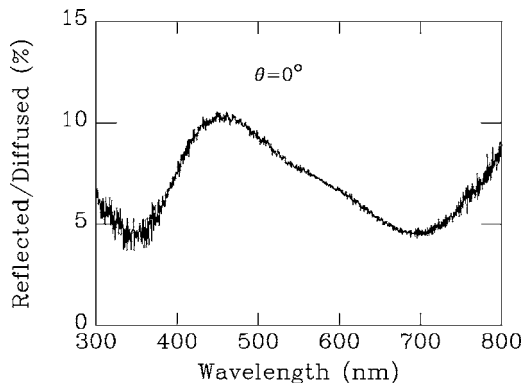


FIG. 3. Spectral distribution of the reflection of white light from blue iridescent feather of *Pica pica*, chosen on the bird's wings. The reflectance spectrum is obtained at an incidence normal to the feather plane (incidence angle  $\theta=0$ ) (450 nm band).

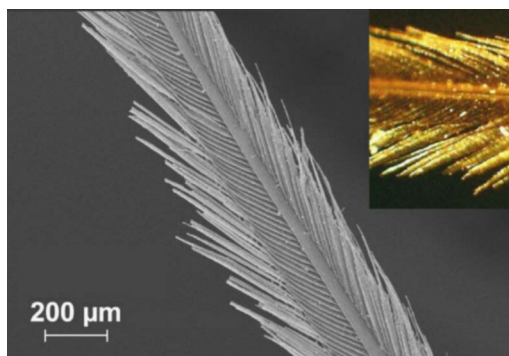


FIG. 4. (Color online) Scanning electron and optical (inset) microscope images of an isolated barb and its attached barbules (not a whole feather). A barbule has the shape of a semirigid ribbon that emerges from the barb with its cross section long side normal to the feather plane. At a few micrometers off the barb, it twists nearly over  $90^\circ$  to orient its flat side in the feather plane.

arises from the barbules (see Fig. 4). A feather has three levels of “barbs.” The central shaft, which gives the longitudinal rigidity to the feather, is the first level. The second level gives the barbs which are attached to the shaft and provides the resistance of the whole feather as an aerodynamic surface. Finally, the barbules, at the third level, are attached to the barbs, and fill the whole feather surface, providing impermeability to air flow and controlling the feather coloration.

The interesting device, from the optical point of view, is then the barbule. The feather has two sides, with different viewing aspects, so that there are different kinds of barbules, and the investigation should be directed to the barbules directly exposed to light and sight. In fact, in a caudal feather of magpie, not all areas of a feather are iridescent. Some of the feathers, entirely visible, show iridescence on both sides of the shaft, while others, half hidden by other feathers, are iridescent only on the visible half. The fact that an organism developing structural colors “economizes” the surfaces where the coloration occurs, accounting for visibility, is not new to magpies feathers. Butterflies such as *Cyanophrys remus*, for instance, are known to display structural colors on the whole ventral side of its wings, but did not develop this coloration on the areas of the forewings that are effectively hidden by the hind wings at all times of rest or flight.

The barbules appear as flat ribbons which are attached to the barbs, normal to the feather plane at the anchoring point. Away from this point, the ribbon twists rapidly over an angle of nearly  $90^\circ$ . This part of the barbules then appear to fill the surface, flat in the feather plane. This is important, because this means that, when viewing a feather along the normal to its shaft-barbs plane, the barbules presents their thickness in the viewing direction, so that the optical device is actually limited in depth. We have investigated the structure of barbules from yellowish-green areas of the tail feathers, and bluish areas of the wings.

Figure 5 shows a barbule from a yellowish-green tail feather, broken in order to reveal its interior structure. This fracture was obtained by simply cutting the feather in liquid nitrogen ( $-196^\circ\text{C}$ ) with scissors beforehand cooled down to

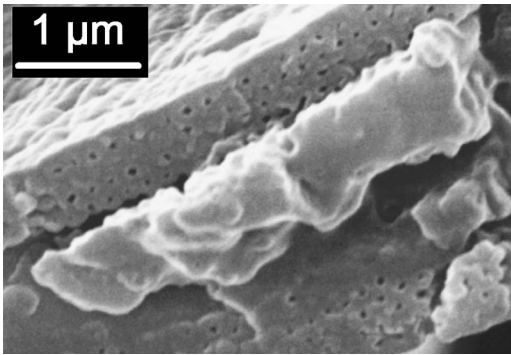


FIG. 5. Cross section of a barbule of a yellowish-green tail feather, showing the cortex surrounding the central core. The cortex is a thin film of keratine and melanine containing cylindrical air holes, regularly distributed.

this temperature. The appropriate direction of cut could easily be determined by optical microscopy. The flat, ribbonlike shape of the barbule is apparent, as well as the separation between the inner core and the outer cortex, which bears the photonic structure. The cortex is a thin layer of an apparently harder material, neatly broken. It has been suggested [11] that this layer, for *Pavo muticus*, should contain pure keratine (of refractive index 1.54) and a similar material containing absorptive melanin, which might bring the refractive index to a maximum value close to 2. We will rely on these numbers for the modeling, below, building on the agreement found in the earlier description of the peacock feather.

A close examination of Fig. 5 reveals the presence of tiny holes in the cortex of the barbule. These holes are arranged on a very coherent two-dimensional hexagonal (i.e., triangular) lattice and have a diameter which can be estimated to be 50 nm. Each hole is neighbored by six other, similar holes, distributed on the summits of a regular hexagon. The distance between two neighboring holes, in any directions, is found to be  $a=180$  nm. In fact, as the inset in Fig. 6 shows, the holes are part of intermediate structures assembled together to form the hard cortex. This intermediate building block is a microtube which, when fully relaxed, spans

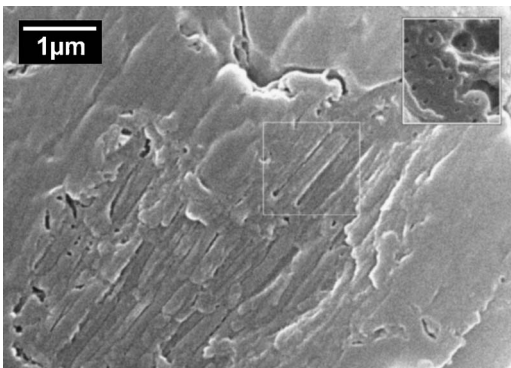


FIG. 6. View of a disaggregated barbule, revealing the longitudinal structure of the cortex (yellow-green feather). The cortex is actually made of fused microtubes (see inset), with an axial empty channel, producing the holes appearing in the cortex sections (Fig. 5). These microtubes are at least  $1.5 \mu\text{m}$  in length.

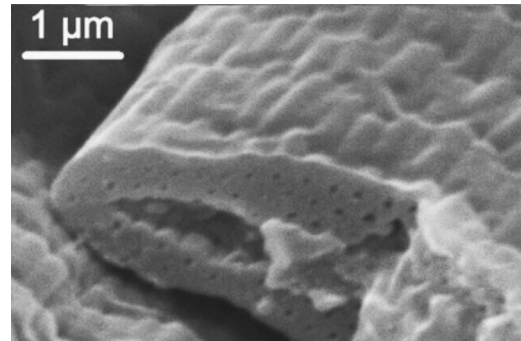


FIG. 7. Cross section of a barbule in a bluish feather from the bird wings. Surprisingly, the distance between the holes in the hexagonal lattice is larger than for the yellowish-green feather.

200 nm in diameter, one quarter of which (50 nm) is occupied by a central empty channel. When fused and packed to form the cortex, these cylindrical microtubes are deformed and compressed to leave no gap between them, so that the cortex appears as a continuous medium containing only the axial holes of the microtubes. In the longitudinal direction, the microtubes have a finite length. This can be seen on the main scanning electron microscope image in Fig. 6, which shows the external cortex surface, damaged by some percussion of the whole feather in liquid nitrogen. In this picture, the microtubes appear to be disaggregated, revealing the longitudinal structure of the barbule cortex. From this, and many similar images, the length of the straight microtubes can be inferred as being in excess of  $1.5 \mu\text{m}$ , i.e., long enough to justify the use of a two-dimensional photonic-crystal model (see, for instance, the length of the long cavities shown inside the white frame, in Fig. 6).

A surprise comes with the examination of the cortex structure of feathers taken from the bird wings. These feathers display bluish reflections and it is expected that the air channels should be closer to each other here, if the mechanisms for the iridescence were similar and a blue shift should be observed. The cortex structure is shown on the electron micrograph in Fig. 7. The same cortex structure and longitudinal cylindrical holes can be seen again, but the measurement of the distance between neighboring holes suggests that the mechanism of production of the iridescence be reconsidered. A careful examination of Fig. 7, and other similar views, indicate a first-neighbors distance of 270 nm, larger than what is found in the case of the yellowish-green cortices. Surprisingly, and contrasting with what was found in the peacock feathers, the shift to shorter wavelengths is not obtained by a reduction of the photonic crystal lattice parameter. This unexpected behavior will be carefully considered in the next section.

Comparing to the better-known peacock feather, we then see several differences: First, *Pica pica* constructs the optical response of its feathers with an hexagonal, rather than rectangular, two-dimensional photonic crystal. Second, the thickness of the cortex layer, measured in units of the neighboring holes separations is much smaller for *Pica pica* than for *Pavo muticus*. And finally, the mechanism of color adjustment (from yellowish-green to bluish) seems to be drastically different in both kinds of birds.

#### IV. DOMINANT REFLECTED WAVELENGTH

In this section, we restrict ourselves to the estimation of the dominant wavelength reflected in the (human) visible range. The cortex of a barbule is, as seen on Figs. 5 and 7, a rather thin layer. However, we deliberately take here a photonic-crystal point of view, as it is known that in thin optical films which are structured by repeating identical patterns, the spectral properties reach very rapidly the “infinite photonic crystal” limit when the number of layers is increased [12]. Also, in this arrangement, the thickness offered to scattered light is limited by absorption, as much as by the geometry. Of course, for more realistic calculations of the detailed reflectance spectrum (see the next section) we will appropriately restrict the thickness of the film.

##### A. Yellowish-green tail feathers

Understanding the reflectance of the yellowish-green barbules requires one to consider the optical properties of the two-dimensional photonic crystal film obtained by drilling air rods in a dielectric material. Assuming, following Li *et al.* [11] that this material contains a high proportion of melanin (which seems reasonable if one considers the black aspect of the feather for off-specular observations), the refractive index should be close to  $n=2$ . In searching for the dominant wavelength, we do not consider the effect of absorption and then neglect the imaginary part of this refractive index, in spite of the presence of this high concentration of melanin.

The distance between the cylindrical holes has been found to be 180 nm. From this, we can infer that, in the cross section of the cortex, the hexagonal lattice primitive cell has a surface area of

$$S = \frac{\sqrt{3}}{2} a^2 = 32\,400 \text{ nm}^2. \quad (1)$$

Each hole has a diameter of  $d=50$  nm, which means that it occupies about 6% of the primitive cell area. The average refractive index can then be estimated to the value  $\bar{n}=1.9$  (this number is obtained from the average dielectric constant and the average inverse dielectric constant, as should be done for unpolarized waves).

With this, we can turn to the estimation of the dominant reflected wavelength. With photonic crystals built with low index contrasts, the directional gaps, in the cross section plane, appear at a given wave-vector  $\vec{k}$ , only if some of its translations  $\vec{k} + \vec{g}$  (by a reciprocal lattice vector  $\vec{g}$ ) falls on the constant-frequency surface

$$\omega = |\vec{k}| \frac{c}{\bar{n}}. \quad (2)$$

This condition allows for the hybridization of plane waves of identical frequencies needed to open a gap at this frequency. It so happen that these set of wave numbers coincide with the boundary of the symmetrized Wigner-Seitz cell of the reciprocal lattice, which is generally used as the first Brillouin zone. Other solutions use the boundaries of the second, third, etc. Brillouin zones, in the repeated zone scheme (see, for instance, Ref. [13]). The choice of one Brillouin zone order

corresponds to the choice of a well-defined frequency gap. The gap frequency should only be retained if it lies in the spectral range of interest, usually the visible range.

The reciprocal vectors of a two-dimensional hexagonal lattice form another hexagonal lattice, and if the distance between the node is  $a$  in the direct lattice, we will find a distance

$$b = \frac{2}{\sqrt{3}} \frac{2\pi}{a} \quad (3)$$

between the nodes of the reciprocal lattice. This means that the boundary of the first Brillouin zone is an hexagon everywhere close to a circle of radius

$$|\vec{k}| = \frac{1}{\gamma'} \frac{2\pi}{a} \quad (4)$$

(determined by identifying the area of the disk with the Brillouin zone area). In this expression,

$$\gamma' = \sqrt{\frac{\pi\sqrt{3}}{2}} \approx 1.65. \quad (5)$$

These relations define the wave vectors where a first-order gap will occur. From the associated frequency, the central wavelength of this gap can easily be determined to be

$$\lambda = \gamma' a \bar{n}. \quad (6)$$

Applying this model to the case of the yellowish-green feather, with  $\bar{n}=1.9$  and  $a=180$  nm, we obtain a value of  $\lambda=564$  nm. This wavelength is only a few percent higher than what has been found experimentally (see Fig. 2), an agreement which strongly suggests that the yellowish-green iridescence is indeed due to the hexagonal lattice of holes in the cortex of the barbules. Within this model, it is also suggested that we have a “first Brillouin-zone boundary gap” reflectance.

##### B. Bluish wing feathers

An attempt to apply the above analysis to the structure found in the blue feathers from the wings leads to the following difficulty: With a measured spacing of  $a=270$  nm between neighboring holes, we would find a gap frequency of  $\lambda=847$  nm, beyond the limit of the visible range, in the infrared. However, in this low-contrast hexagonal structure, there is a higher gap, which corresponds to a wave-vector norm that reaches the second Brillouin zone, also of hexagonal shape. The argument above can be repeated with this larger Brillouin zone, with the result that the reflection wavelength is

$$\lambda = \gamma' a \bar{n}, \quad (7)$$

with

$$\gamma' = \frac{\gamma'}{2}. \quad (8)$$

The “second Brillouin zone” reflectance wavelength is just one half of the first Brillouin zone wavelength. With a holes

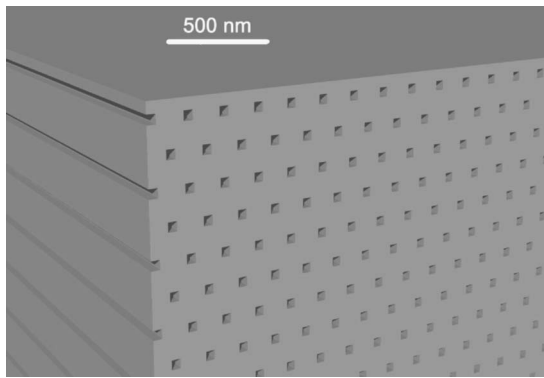


FIG. 8. Model of the structure used for the numerical calculation of the reflected spectrum. The two-dimensional photonic crystal is actually an homogeneous block of keratin and melanin (refractive index 2) which contains an hexagonal lattice of parallel air channels. The distance of neighboring holes (for a yellowish-green feather) is 180 nm, while the size of the holes is 50 nm (50 nm  $\times$  50 nm for a square section). The light is incident on this structure along the normal to the horizontal surface, above the structure.

interdistance of  $a=270$  nm, we get 423 nm (half the value of 847 nm). This is in the greenish blue part of the visible spectrum. In view of the fact that we neglected the confining effect due to the finite thickness of the cortex, this second Brillouin-zone boundary gap reflectance could plausibly be the origin of the blue iridescence of the wing feathers. However, in that case, it should be expected to also see a strong reflectance in the infrared, near 847 nm. Attempts to detect this infrared reflection have failed, and the wings of the magpie do not seem to display a bright “near-infrared” color. A more elaborate model, accounting for the finite thickness of the cortex should be developed in order to conciliate these findings.

We should note that a simple Fabry-Pérot explanation alone (accounting for a thickness  $d=1$   $\mu$ m of the cortex) is not likely to provide a simple explanation of the reflectance spectrum: a thin film with an average refractive index of  $\bar{n}=1.9$ , impacted by white light under normal incidence, would give reflectance resonances at wavelengths  $\lambda=(2d\bar{n})/(m+\frac{1}{2})$ . This leads to several resonances covering the visible range, and more should be found in the infrared region. This, again, is not observed.

## V. COMPUTED REFLECTANCE SPECTRA

The above estimations of the dominant wavelength can be confirmed by detailed calculation of the reflectance spectrum. A transfer matrix technique [14] can be used to compute the three-dimensional electromagnetic multiple scattering leading to precise reflection coefficients.

Figure 8 summarizes the geometry of the dielectric model used in the calculation. Pure keratin has a refractive index of 1.54 [15], but the material in the cortex [11] is believed to have a higher refractive index, closer to the value  $n=2$ , indicating a high proportion of melanin [16]. As mentioned above, the presence of a large quantity of melanin is confirmed by the black appearance of these feathers under most

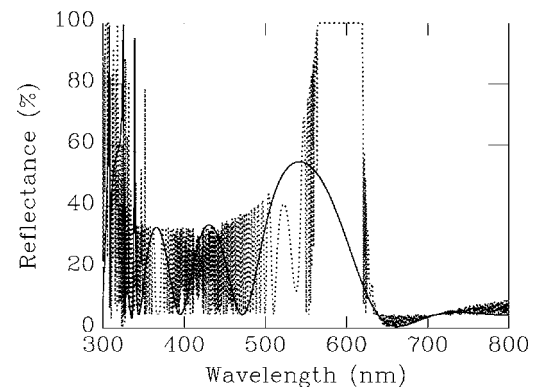


FIG. 9. Reflectance spectrum (dotted line) calculated for two-dimensional model shown on Fig. 8. The distribution of cylindrical pores is an hexagonal lattice, with a nearest-neighbors separation of 180 nm. The solid line is the same calculation, when the cortex is more realistically represented by a photonic crystal film of three normal periods.

illumination conditions. Also, it can be observed that the incidental disappearance of the melanine pigment seems to destroys the barbule structure: Albino magpies exist (one of them is on display at the Natural History Museum in London) and this bird does not show the iridescence studied here. The question of the exact location of melanin in the barbule section is, however, a difficult question, still worth a detailed study.

Reflectance spectra have been considered for half-space bulk photonic crystals, and for more realistic photonic-crystal films. The cylindrical holes are replaced, in the calculation, by prismatic cavities with a square-shaped cross section. This approximation has no consequence, as the size of the modifications is much smaller than the wavelength of the filtered radiation. The advantage of this slight transformation is that the number of transfer matrices to be calculated and stored is considerably reduced, easing the numerical calculation, and thereby making it much more reliable.

The spectra resulting from a simulation of the optical properties of the tail feather are shown in Fig. 9. The large total reflection band appears correctly in the yellowish-green region, slightly above the observed 550 nm band, for the semi-infinite structure (dotted line) and very near this frequency for a structure reduced to a two-periods film (solid line). The side oscillations found in the “infinite” structure reflectance are due to spurious Fabry-Pérot standing waves, which develop because the calculation was actually carried out with a very thick film (512 periods) rather than on an exact ideal semi-infinite photonic crystal. The reflection resonance found for the finite-thickness film reproduces quite well the observed dominant wavelength, even if the infinite model seems to be slightly off.

Figure 10 shows the result of a simulation of the bluish cortex feather reflectance. The dotted line is similar to the model considered above for the yellowish-green barbules, with a very thick film (512 periods) and no absorption. This spectrum fully confirms the estimations given above for the location of the reflectance bands. The large band close to 900 nm originates in the first Brillouin zone gap, while the

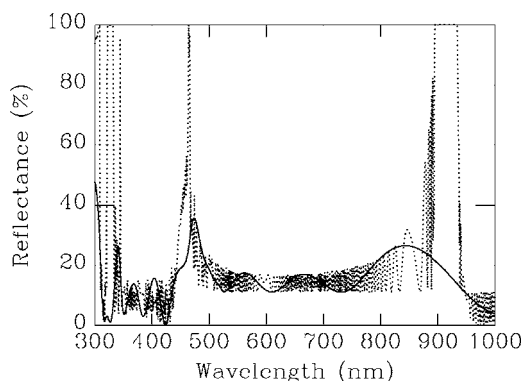


FIG. 10. Reflectance spectrum calculated for the photonic crystal film model of the bluish feather cortex of *Pica pica*. The dotted line refers to a quasi-infinitely thick film (precisely, 512 normal periods), while the solid line refers to a film containing only two periods.

band near 450 nm, responsible for the blue coloration, arises from the second Brillouin zone boundary, as explained above. “Seeing” the large reflectance in the infrared (even when equipped with adequate near-infrared detectors) is not obvious, because of the very limited thickness of the barbule cortex. The solid line in Fig. 10 is a calculation based on the two-dimensional photonic-crystal model, but the thickness of the reflecting film is limited to two periods. This calculation shows that the contribution to the reflectance close to 900 nm becomes much more discreet, while the contribution at short visible wavelengths is somewhat more robust.

It could be argued that this simulation might eventually only contain Tyndall scattering, and not photonic-crystal effects, as the thickness of this photonic crystal is so small. The difference is that Tyndall scattering refers to the action of isolated scatterers, contrasting the collective, photonic-crystal behavior. This is actually not the case for the blue scattering: If, in the film reflectance calculation, the distance between the cylindrical pores is increased by 10%, the blue reflectance band is seen to also shift towards 10% longer wavelengths. This shows that the collective arrangement of holes is the primary cause of the blue coloration, with changes on the shape or size of the holes being much less effective to modify the reflectance spectrum.

## VI. CONCLUSION

Though less spectacular than the bright colors of a male peacock, the coloration of some of the feathers of the common magpie is generated by a similar process: a two-dimensional photonic crystal formed by parallel air channels in the cortex of the barbules. For some reason, the lattice has evolved to be hexagonal, rather than the previously known rectangular lattice. Contrasting the mechanism for coloration of the peacock feather, different colorations are not obtained by the expected rescaling of the characteristic lengths in the structure.

The yellowish-green reflection seen on the tail of the magpie can easily be explained by a photonic-crystal “first-

gap” effect. This mechanism has been seen on other feathers and, in particular, has been suggested for explaining the coloration of the peacock tail. The blue reflections from the wings is actually more subtle, because it involves a photonic-crystal “second-gap” effect, complemented by the avoidance, by confinement, of the first-gap infrared reflection.

The photonic devices found on living organisms are known to cover a very wide range of functions. For instance, control of thermal radiative exchange has been recognized in several instances [17], and ultraviolet protection has also been suggested [18]. The best known function is, however, coloration [19], which participates in conspecific recognition, including improving chances of male and female interaction for mating, and plays a crucial role in the competition between prey and predators.

Magpies, like other Corvidae, are sexually monomorphic in terms of their plumage color, and males and females alike possess iridescent tail feathers [1,20]. The biological significance of tail coloration is thought to be related to both intra- and intersexual interactions because of its prominent display in both contexts [1,20]. Such a display is termed passive “wing-flirting” and involves lowering the head and lifting the wings and tail to between 30° and 40° above the back [21]. Studies of the role of the tail in sexual selection, in particular, have revealed that it may be used by females in mate selection, and males with less damaged (and presumably brighter iridescent) tails, have been found to be more likely to form pairs and fledge offspring [22].

In relation to this, it should be noted that the present paper focusses on the coloration of a bird as we (humans) perceive it. Human classification of colors is limited by the trichromatic structure of our retinal receptors, and the specific spectral range of each of the red, green, and blue stimuli that activate the color interpretation. The spectral range discussed in this paper has then often been restricted to the human visible range, from 380 nm to about 770 nm. However, most spectroscopic data, measured or computed, include some near ultraviolet region and the content of ultraviolet light in the magpie plumage, shown on reflectance measurements and in simulations, is not negligible (see Figs. 2, 3, 9, and 10, between 300 nm and 400 nm). Most probably, data restricted to human perception are not complete enough to allow stepping into many important biological questions, such as assessing the purpose (cryptic, defensive, signaling, etc.) of the colored patterns which has been described. All the living species which interact with the magpie are not concerned by human limitations. As an example, many birds are known to have developed ultraviolet cones, which make their color perception tetrachromatic rather than trichromatic. In such a colorimetric space, even the anthropocentric naming of the colors would be inappropriate. This means that the reduction of our vision system leaves us in a world in which many visual messages from our environment are not reaching us. From theoretical considerations, this work suggests that the magpie could be sending some of these messages, still to be decrypted.

## ACKNOWLEDGMENTS

This investigation was conducted with the support of the European BioPhot (NEST) project, under Contract No.

12915. The authors thank Thierry Tancrez for allowing them to use the photograph in Fig. 1 for illustration purposes, Van Tendeloo for his invitation to use the JEOL JSM 5510 of the EMAT Center (University of Antwerp), and Amand Lucas (FUNDP) for enlightening discussions. This work was carried out with support from EU5 Centre of Excellence ICAICT-2000-70029 and from the Inter-University Attraction Pole (IUAP P5/1) of the Belgian Office for Scientific, Tech-

nical, and Cultural Affairs. It was also partly supported by the European Regional Development Fund (ERDF) and the Walloon Regional Government under the “PREMIO” INTERREG IIIa project. The authors acknowledge the use of Namur Interuniversity Scientific Computing Facility (Namur-ISCF) for the numerical simulations. V.L. and J.F.C. also acknowledge support from the Belgian National Fund for Scientific Research (FNRS).

- 
- [1] S. Cramp and C. M. Perrins, *The Birds of the Western Palearctic. Handbook of the Birds of Europe, the Middle East and North Africa* (Oxford University Press, Oxford, 1994).
- [2] L. Auber, Proc. Zool. Soc. London **129**, 455 (1957).
- [3] L. Auber, Proc. R. Soc. Edinb **74**, 27 (1971).
- [4] T. Nissen, Mikroskopie **13**, 1 (1958).
- [5] R. O. Prum, R. H. Torres, S. Williamson, and J. Dyck, Nature **396**, 28 (1998).
- [6] A. Mallock, Proc. R. Soc. London **A85**, 528 (1911).
- [7] E. Merritt, J. Opt. Soc. Am. **11**, 93 (1925).
- [8] J. Dyck, Z. Zellforsch Mikrosk Anat. **115**, 17 (1971).
- [9] J. Dyck, Biol. Skrifter **18**, 5 (1971).
- [10] J. Zi, X. Yu, Y. Li, X. Hu, C. Xu, X. Wang, X. Liu, and R. Fu, Proc. Natl. Acad. Sci. U.S.A. **100**, 12576 (2003).
- [11] Y. Li, Z. Lu, H. Yin, X. Yu, X. Liu, and J. Zi, Phys. Rev. E **72**, 010902(R) (2005).
- [12] J. M. Vigoureux and F. Baida, Opt. Commun. **101**, 297 (1993).
- [13] J. M. Ziman, *Principles of the Theory of Solids*, 2nd ed. (Cambridge University Press, London, 1972).
- [14] J. B. Pendry and A. MacKinnon, Phys. Rev. Lett. **69**, 2772 (1992).
- [15] J. Dyck, Z. Zellforsch Mikrosk Anat. **115**, 17 (1971).
- [16] M. F. Land, Prog. Biophys. Mol. Biol. **24**, 75 (1972).
- [17] L. P. Biró, Z. Bálint, K. Kertész, Z. Vértésy, G. I. Márk, Z. E. Horváth, J. Balázs, D. Méhn, I. Kiricsi, V. Lousse *et al.*, Phys. Rev. E **67**, 021907 (2003).
- [18] J. P. Vigneron, M. Rassart, Z. Vértésy, K. Kertész, M. Sarrazin, L. P. Biró, D. Ertz, and V. Lousse, Phys. Rev. E **71**, 011906 (2005).
- [19] S. Berthier, *Iridescences, Les Couleurs Physiques des Insectes* (Springer-Verlag, Paris, 2003).
- [20] C. J. F. Coombs, *The Crows: A Study of the Corvids of Europe* (Batsford, London, 1978).
- [21] D. Goodwin, British Birds **4 XLV**, 113 (1952).
- [22] S. Fitzpatrick and P. Price, Behav. Ecol. Sociobiol. **40**, 209 (1997).